sciendo
Polish Journal of Medical Physics and Engineering
The Journal of Polish Society of Medical Physics
ISSN 1898-0309, doi: 10.2478/pjmpe-2024-0019
September 2024
Vol 30, Issue 3

Scientific Paper

Investigation of the impact of local properties of 3D data on the accuracy of block matching-based speckle tracking echocardiography

Szymon CYGAN [1,ABCDEF,*], Aleksandra WILCZEWSKA [1,CEF], Tomasz KUBIK [2,BCE], Martino ALESSANDRINI [3,ABE]
[1]*Institute of Metrology and Biomedical Engineering, Faculty of Mechatronics, Warsaw University of Technology, Warsaw, Poland*
[2]*PMOD Technologies LLC, Fällanden, Switzerland*
[3]*Cardiovascular Imaging and Dynamics, KU Leuven, Leuven, Belgium*
Corresponding author: Dr. Szymon Cygan; szymon.cygan@pw.edu.pl

(received 14 March 2024; revised 17 June 2024; accepted 15 July 2024)

Abstract

Introduction: Due to its simplicity, block-matching is a popular motion-tracking method used in speckle-tracking echocardiography. Improvement of its robustness and accuracy is thus of prime interest. Although it seems plausible that the quality of block matching-based tracking depends on the local properties of image data, and thus, it should be possible to assess in advance how well certain portions of the image data are suited for displacement estimation, the potential relationship has not been studied extensively.
Material and methods: This study aimed to search for a relationship between selected features of echocardiographic data and the quality of local displacement estimation. The study used a 3D synthetic B-mode imaging sequence data with known ground truth. Frame-to-frame displacements were estimated for 9856 points in five different frame pairs with mean inter-frame displacements of 0.15, 0.87, 2, 3.02, and 3.84 mm. In each case, tracking errors were evaluated against thirteen grayscale image features, the displacement's magnitudes, and the normalized cross-correlation (NCX) values. Additionally, a multi-variable regression model was applied to test the combined ability of the proposed features to predict tracking quality.
Results: Median tracking error magnitudes were 0.06, 0.13, 0.28, 0.74, and 1.5 mm for each image pair. Weak correlation between errors and individual data features was found only in the case of 3 features: NCX (Pearson's correlation coefficients in the range of -0.366 to -0.223), number of speckles within the kernel (-0.283, -0.282, and -0.214 for three lowest deformations) and mean of the 3D gradient (-0.252, -0.237 and -0.25). The regression model, however, provided significant prediction improvement with R^2 exceeding 0.5.
Conclusions: In conclusion, only a weak relationship between the individual investigated kernel features and tracking accuracy has been established, but their combined strength can be assessed as at least moderate.

Keywords: 3D echocardiography; speckle tracking echocardiography; strain imaging; block matching.

Introduction

Speckle tracking echocardiography (STE) employs a variety of motion-tracking methods, with block matching (BM) being a popular approach.[1] While it is reasonable to assume that the tracking quality in specific areas of the image is influenced by the features of the input data (i.e., the underlying image), the relationship between the two remains unexplored, as indicated by an earlier study.[2]

Searching for such a relationship requires input data with known ground truth. In the process of validation and verification of echocardiography strain imaging methods, four major approaches are available[3]:

1. Clinical data obtained from two modalities[4], where in most cases, echocardiography is paired with MRI;
2. Data from animal models that can be paired with MRI or sonomicrometry;
3. Phantom-based data acquisitions,[5-7] where significant control over the experimental conditions is possible and the results can be paired with sonomicrometry or numeric simulations;
4. The utilization of synthetic data[1,8] generated based on a numerical model of the examined tissue.

Authors' contribution: A – Research concept and design, B – Collection and/or assembly of data, C – Data analysis and interpretation, D – Writing the article, E – Critical revision of the article, F – Final approval of the article.

The first approach provides the most realistic conditions. At the same time, the last provides the most extensive ground truth information, making it the only solution suitable for quantitative evaluation of tracking performance on a local scale.[9,10]

STE is performed by tracking the selected points of the image of the myocardium throughout the cardiac cycle. Selecting the points to be tracked can be based on various criteria. First, the points need to be located within the myocardium as the object of interest.[11] Region of interest can be either user-defined or segmented automatically. It is possible to track all the data pixels or voxels within the region of interest, but this approach is computationally challenging and thus inefficient. In most approaches, the selection of points is based on the ventricle geometry[12] and connected with the endocardial and epicardial borders and with the myocardial midline as well as with the applied ventricle segmentation scheme (usually 16, 17, or 18-segment standard).[11]

Contribution of this study

This study aims to increase the accuracy and robustness of block-matching-based 3D speckle-tracking echocardiography methods. For this purpose, we investigate if it is possible to predict how well a block-matching-based displacement estimation method will perform for a particular point of the input data based on local features of the echocardiographic data. We examine the correlation between several metrics calculated for the 3D data blocks used for matching and resulting displacement estimation errors. By selecting features that correlate with tracking errors, it is possible to enhance the accuracy of displacements and strain estimation. This enhancement can be achieved through the appropriate preselection of tracking points or by evaluating the reliability of predefined points, potentially resulting in reduced estimation errors.

Materials and methods

Synthetic data

This study used 3D synthetic echocardiographic B-mode imaging sequence data with known ground truth. The normal (healthy) case, without pericardium, provided in the Straus study[8], was selected.

As an initial ventricle geometry, a numerical heart model was created in the abovementioned study using a natural heart anatomy segmented from a magnetic resonance imaging examination. The model consisted of tetrahedral finite elements defined by 9856 nodes. A Bestel-Clement-Sorine electromechanical model of the heart was used to simulate the myocardium deformation.[13] A fast ultrasound simulator COLE produced the three-dimensional B-mode image sequence.[14] The data featured a frame rate of 30 Hz thanks to parallel beam forming. After mapping to a Cartesian coordinate system and cropping, the final data sets consisted of 297×297×297 isotropic voxels with a size of 0.3367 mm and an 8-bit resolution. **Figure 1** presents the first volume of the data in three mutually perpendicular cross-sections. The same numerical model of the left ventricle was used to generate more realistic synthetic echocardiographic data than the one used in ref. 15. This data has been made available for studies like the one presented here. However, we selected the earlier, more straightforward version since it provided a wider field of view (FOV), enabling tracking all available reference points.

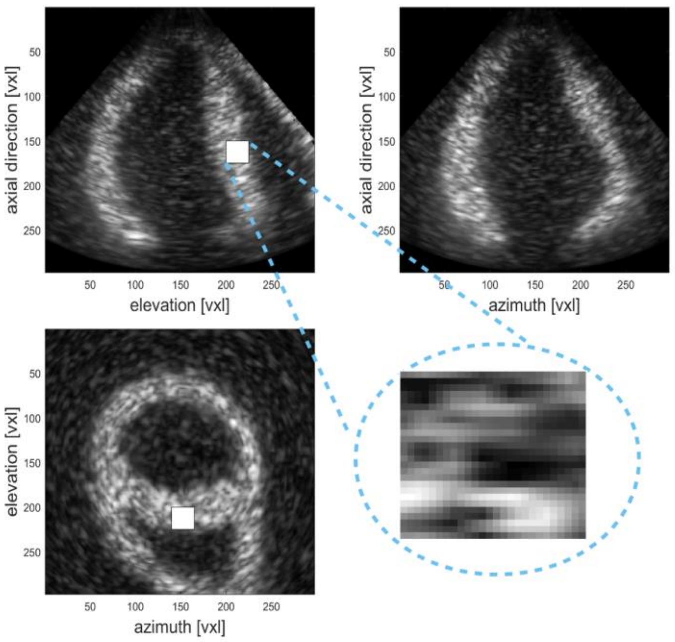

Figure 1. Mutually perpendicular cross sections of the volumetric, synthetic 3D data of the LV model, with example kernel marked in white. Enlarged – 2D section of the kernel.

In order to assess the possible impact of the features of the data within the tracked block on the estimation errors, without the influence of possible errors occurring at previous data frames, we estimated only the frame-to-frame displacements in this study. Furthermore, five different pairs of frames, taken from the systolic phase of the cardiac cycle, were used in this study to obtain different frame-to-frame displacement magnitudes. From the 27 frames covering the cardiac cycle, displacements were estimated between frames 1 and 2, 4 and 5, 4 and 6, 4 and 7, and finally 4 and 8, providing mean inter-frame displacements of 0.15, 0.87, 2.00, 3.02, and 3.84 mm respectively (**Figure 2**). The first pair corresponds to the original data frame rate of 30 Hz and minimal deformation in the LV model just prior to contraction of the myocardium. The second pair corresponds to the contraction phase and, thus, the maximum deformation rate, registered at the initial framerate of 30 Hz. The rest of the pairs were also selected from the contraction phase but corresponded to a lower framerate of 15, 10, and 7.5 Hz, respectively. Such frame rates are considered too low for STE, and the purpose of using such a setting here was to worsen the conditions of block matching artificially.

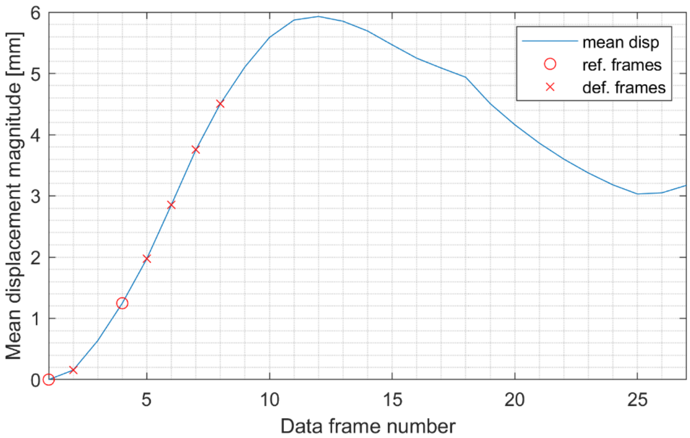

Figure 2. Ventricle deformation cycle presented as nodes mean displacement. 'Ref. frames' mark the frames used as reference frames and 'def. frames' denotes the deformed frames used for displacements estimation.

Displacement estimation method

We have used a 3D block matching algorithm to assess the intrinsic tracking quality, previously tested in a comparison study[1]. It is a simplified method, which generated slightly higher errors than three out of five methods tested in the mentioned study. However, its simplicity and lower computational cost make it a good fit for the purpose of this study.

The main difference between the algorithm applied in this study and the one described before is that the algorithm here is used with neither temporal nor spatial regularization, which was excluded from the method in order to study the tracking quality at every point independently. The method uses a cubic 8.4 × 8.4 × 8.4 mm kernel to calculate displacements of the given points – an example of the kernel and its enlarged visualization are presented in **Figure 1**. The size of the kernel was selected for this particular data set. Search range dimensions were defined so that they allow for maximum frame-to-frame displacement corresponding to 120 mm/s tissue velocity. A normalized cross-correlation function (NCX) was used as a similarity metric. In order to achieve sub-voxel resolution (1/16 of a voxel), the metric function was interpolated using a three-dimensional cubic B-spline method. For each image pair, all nodes of the underlying numerical heart model (9856 points) were tracked, and the corresponding tracking errors were calculated as a magnitude of position differences between the tracking results and the numerical heart model reference points.

Evaluation

Feature set

As an attempt to identify features or metrics of the tracked data blocks, that might correlate with the quality of tracking, the following gray scale based metrics of the kernel were calculated. For the convenience of the reader, they have been divided into four groups (A through D):

A. *B-mode data based metrics*:

1. Mean value of the voxel intensities within the kernel block.
2. Variance of the voxel intensity values within the kernel block.
3. Skewness of the histogram of voxel intensity values within the kernel block.
4. Kurtosis of the histogram of the voxel intensity values within the kernel block.

B. *Metrics of the 3D gradient of the data*:

5. Mean of the 3D gradient magnitude of the voxel intensity values within the kernel block.
6. Variance of the magnitude of the 3D gradient within the kernel block.
7. Skewness of the histogram of the magnitude of 3D gradient within the kernel block.
8. Kurtosis of the histogram of the magnitude of 3D gradient within the kernel block.

C. *Metrics of the binarized 3D gradient of the data*:

9. Sum of a binarized magnitude of the 3D gradient of the kernel block, where binarization was carried out by thresholding with a relative threshold of 0.5.
10. Sum of a binarized magnitude of the second-order 3D gradient of the kernel block.

D. *Speckles characterization via thresholding*:

11. The number of speckles within the block, where speckles were labeled after segmentation carried out by thresholding with a relative threshold of 0.66.
12. The size of the largest speckle, where the size is the number of voxels in this speckle obtained from segmentation.
13. Mean speckle size in the kernel block.

All the histograms consisted of 50 bins for grouping the intensities of the evaluated data. Additionally, the following metrics relating not only to the initial frame of the data, but to the process of tracking, were calculated (constituting the fifth group E):

E. *Frame-to-frame changes in the data:*

14. The displacements magnitude.
15. The maximum value of the block-to-block similarity metric used for block-matching: the normalized cross-correlation function.

Correlation and linear regression

As a result, for every tracking instance (all the points in all frame pairs), values of all the above-mentioned metrics for the first-frame block were obtained. Possible correlations between tracking errors and those metrics were evaluated for each frame pair separately by calculating Pearson's correlation coefficients (corr) for each case and fitting linear models whose coefficients of determination (R^2) were calculated.

F-test

As a complementary means of evaluation, the individual importance of each of the features was assessed using the *F*-test algorithm.[16] A hypothesis that the response values grouped by predictor feature values are drawn from populations with the same mean was tested against the alternative hypothesis that the population means are not the same. The resulting scores used for the evaluation of the significance of each feature were calculated as *-log(*p*-value)* of the *F*-test.

Multi-variable regression

In order to test the ability of the proposed features to collectively enable an improved prediction of the tracking quality, a machine learning regression model was trained using the obtained feature sets with the displacement estimation errors used as the reference response. An ensemble of bagged decision trees model was used with minimum leaf sizes of 8 and 30 learners. Out of the 9856 tracked points, 15% were excluded as a test data set for evaluating the trained model.

Group E of the proposed features takes into account the changes in data from one frame to another. Apart from the model that incorporates all the features, we conducted another regression training and testing procedure specifically for the features belonging to groups A through D.

Another series of regression model training was performed while reducing the number of features used based on the results of the F-test. Subsequent ensemble-type models were trained to start from the original 15 features to the two most relevant according to the F-test. The R^2 values for each model evaluated for the 15% test data set were obtained.

Results

The mean and median tracking error magnitudes obtained for the five examined volume pairs with different mean inter-frame displacement magnitudes are presented in **Table 1**.

Table 1. Mean and median displacements estimation errors for each case of mean interframe displacements.

Mean displacement [mm]	0.15	0.87	2.00	3.02	3.84
Mean estimation error [mm]	0.07	0.50	1.08	1.92	2.50
Median estimation error [mm]	0.06	0.13	0.28	0.74	1.50

Correlation and linear regression

Values of Pearson's correlation coefficients and the coefficients of determination R^2 for all the examined metrics and the displacement cases are presented in **Table 2**. All the correlation cases with absolute values exceeding 0.2 are underlined in the table, suggesting a weak correlation between the examined value and the estimation error.[17]

Table 2. R-squared (R^2) and Pearson's correlation coefficient (corr) values for displacement estimation errors vs. all the data features examined for all mean inter-frame displacements. Bolded cases are represented in Figure 3, underlined are values of correlation coefficients exceeding 0.2 or -0.2.

Mean disp.		0.15 mm		0.87 mm		2.00 mm		3.02 mm		3.84 mm	
Gr.	**Feat.**	**R^2**	**corr**	**R^2**	**corr**	**R^2**	**corr**	**R^2**	**corr**	**R^2**	**corr**
A	1	0.004	0.067	0.007	0.084	0.001	0.036	0.003	0.054	0.001	-0.036
	2	0.000	0.016	0.019	-0.137	0.066	-0.257	0.049	-0.222	0.030	-0.174
	3	0.001	0.032	0.019	0.138	0.050	0.223	0.033	0.182	0.009	0.095
	4	0.007	0.082	0.016	0.127	0.043	0.206	0.020	0.141	0.003	0.057
B	5	0.063	-0.252	0.056	-0.237	0.062	-0.250	0.013	-0.114	0.001	-0.022
	6	0.010	-0.098	0.008	-0.087	0.019	-0.137	0.005	-0.068	0.003	-0.059
	7	0.053	0.229	0.062	0.248	0.033	0.182	0.005	0.072	0.004	-0.060
	8	0.028	0.167	0.030	0.174	0.022	0.149	0.005	0.073	0.000	-0.016
C	9	0.021	-0.145	0.028	-0.168	0.011	-0.103	0.001	-0.024	0.004	0.064
	10	0.001	-0.038	0.000	-0.004	0.003	0.054	0.003	0.056	0.004	0.062
D	**11**	**0.080**	**-0.283**	**0.079**	**-0.282**	**0.046**	**-0.214**	**0.005**	**-0.071**	**0.000**	**0.021**
	12	0.003	0.057	0.004	0.061	0.000	-0.022	0.000	0.007	0.000	-0.007
	13	0.005	-0.068	0.006	-0.077	0.009	-0.097	0.000	-0.006	0.000	0.011
E	14	0.115	0.340	0.008	-0.090	0.008	-0.091	0.044	-0.210	0.067	-0.259
	15	**0.134**	**-0.366**	**0.156**	**-0.395**	**0.118**	**-0.343**	**0.092**	**-0.303**	**0.050**	**-0.223**

For visual inspection of obtained results, scatter plots of each metric and mean inter-frame displacement were created during the examination. **Figure 3** presents, as an example, estimation errors vs. the number of speckles within the tracked block (upper row) and the estimation errors vs. the maximum NCX values registered during displacement estimation (bottom row). Instead of scatter plots, bins holding the central 66% of the points in their ranges are shown along with plots of mean and median values and the linear model fitted to the data.

F-test

Results of the evaluation of the individual importance of each feature for the displacement estimation errors as assessed by the F-test are presented in **Table 3**. Higher score values indicate a stronger significance of the feature for prediction.

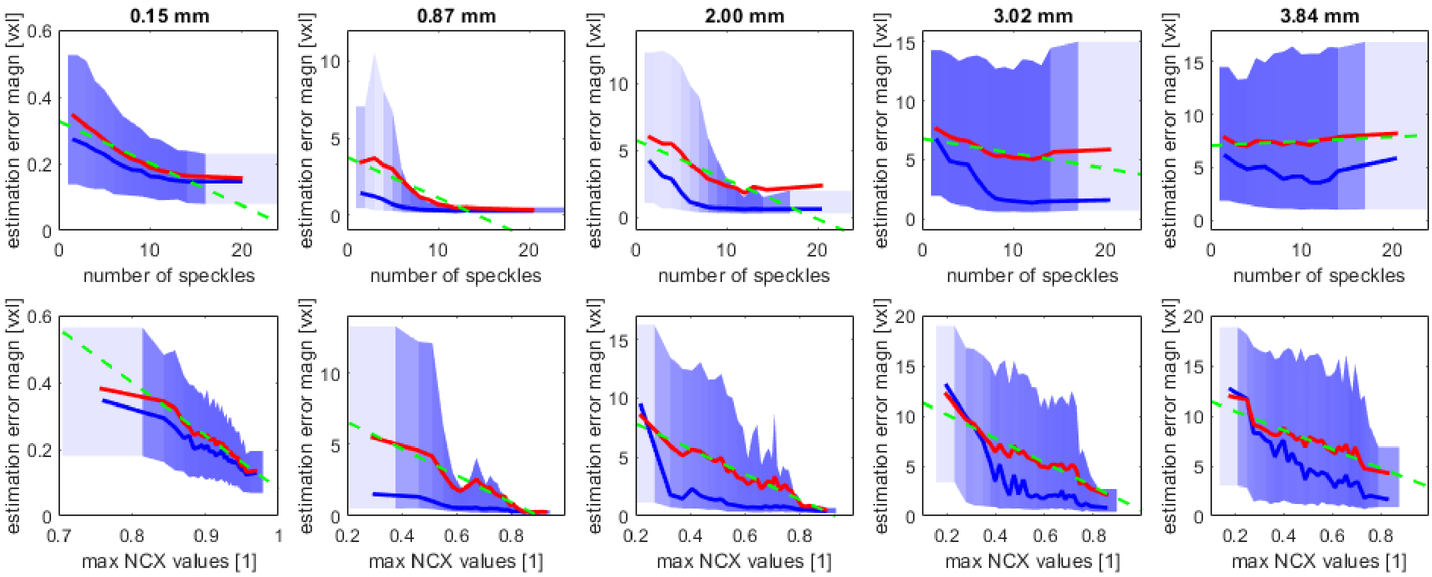

Figure 3. Binned plots of the estimation error magnitudes versus the number of speckles within the kernel (top row) and the maximum of the normalized cross-correlation function (bottom row). The blue lines are the median in each of the 32 equinumerous bins, red – mean value, the shaded area – the range covering middle 66 percentiles of results with shading transparency corresponding to the number of values registered in given bin over its area. Dashed green line is the linear model fitted to the data.

Table 3. F-test scores for each feature used, calculated separately for all mean inter-frame displacements. Colors from green to red highlight estimated relevance of each feature for each mean displacement separately.

Group	Feat.	0.15 mm	0.87 mm	2.00 mm	3.02 mm	3.84 mm
A	1	153.6	76.23	79.11	178.2	136.4
	2	57.15	211.9	320.3	220.6	131.2
	3	11.11	90.4	209	140.6	29.86
	4	46.42	103.5	160	71.16	5.799
B	5	435.8	450.3	304.1	48.97	16.49
	6	127.2	124.2	74.68	39.71	45.5
	7	276.4	301.6	123.5	14.316	22.71
	8	305.6	329	147.18	28.73	21.67
C	9	92.02	106.1	34.71	1.78	8.901
	10	14.82	0.6649	8.049	7.382	9.619
D	11	356.3	404.3	232.3	36.38	2.533
	12	47.79	11.71	4.264	4.338	1.777
	13	58.18	43.03	32.98	1.206	4.112
E	14	466.6	66.87	73.27	274.1	373
	15	561	716.7	512	398.8	201.5

Table 4. Values of RMSE and R^2 obtained for the test data fed to the trained regression models for all the features from groups A to E and for features from groups A to D.

Features	0.15 mm		0.87 mm		2.00 mm		3.02 mm		3.84 mm	
	RMSE	R^2	RMSE	R^2	RMSE	R^2	RMSE	R^2	RMSE	R^2
A to E	0.1057	0.493	2.068	0.532	3.786	0.399	5.046	0.36	5.846	0.28
A to D	0.1065	0.485	2.086	0.524	3.779	0.401	5.066	0.35	5.861	0.277

Multi-variable regression

The results of regression training and testing using the 15% test data sets were evaluated based on obtained root mean square errors (RMSE) and coefficients of determination (R^2). The resulting values are given in **Table 4**.

Figure 4 presents how the models' performance measured by the R^2 depends on the number of features used. The features were selected as ordered by descending F-test results values.

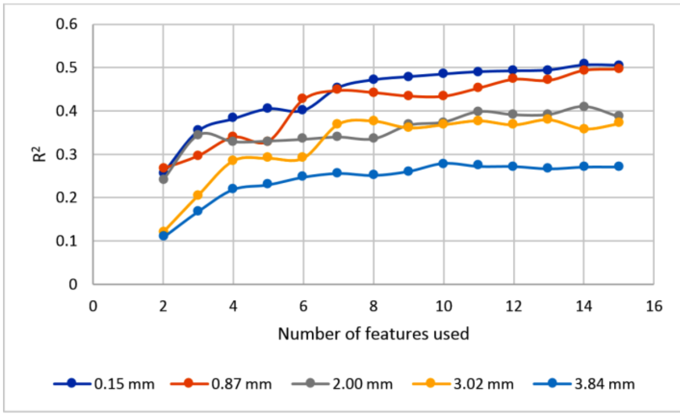

Figure 4. R^2 obtained for regression models depending on the number of features used – separate plots for each mean displacement case.

Discussion

Obtained mean tracking error magnitudes for each examined image pair (0.07, 0.5, 1.08, 1.92, and 2.5 mm mean displacement, respectively) are significant compared to the mean displacements between those frames. Mean relative errors were 45%, 57%, 54%, 64%, and 65%, respectively. Large values of mean errors can be partially explained by poor displacement tracking in the basal segments of the ventricle data, which was the reason for excluding this area from the original Straus study.[8] Median displacement tracking errors for the 5 cases here are 0.06, 0.13, 0.28, 0.74, and 1.50 mm, respectively, comparable to the original study's results.

As shown in **Table 2**, Pearson's correlation coefficients do not show any strong or moderate relation between estimation errors and examined metrics. Weak correlations with the absolute value of Pearson's correlation coefficient in the range of 0.2 – 0.4 were marked in **Table 2** by underlining the coefficient value. It can be noted that for smaller frame-to-frame deformations, the results show a weak correlation between estimation errors and the mean value of the 3D gradient of the data kernel block used for block matching (metric 5) and the skewness of the histogram of the 3D gradient of the data kernel block (metric 7). A slightly stronger, although still weak, correlation can be observed in the number of speckles identified in the reference kernel block (metric 11), which can also be seen in the plots in **Figure 3** (first 3 cases in the upper row). A larger number of speckles visible in a single data block means that the variability of voxel values within the examined block is higher. So, higher gradient values can be present. A larger number of speckles visible in a single data block (metric 11) means that the variability of voxel values within the examined block is higher. So, higher gradient values can be present (metric 5). The fact that both these features show some correlation with estimation error values is in agreement with results reported in ref. [2], where strain estimations have been more accurate in areas with higher amounts of edges.

The last two metrics (numbers 14 and 15) use the comparison between the reference kernel and the frame acquired after deformation. In a standard setting, only the value of the similarity metric is available (here, the maximum of the NCX function), and the information on the actual displacements is not. The obtained results show that the value of the normalized cross-correlation function used for block matching shows a weak correlation with the magnitudes of displacement estimation errors. Correlation is weak but most significant among the obtained values, presented in **Table 2**.

Interestingly, the correlation between the tracking errors and the displacement magnitude is inconsistent throughout the cases examined as the sign of correlation coefficient changes from positive for the lowest mean displacement to negative (increasing in magnitude) with increasing mean displacement. This inconsistency is likely because other data features in each pair influence estimation more strongly than displacements. For instance, the location of the point to be tracked in the field of view and, thus, the distance from the focal point of the ultrasonic beam may influence the tracking more than the displacement magnitude. In the vicinity of the focus, one can expect a finer speckle pattern in the ultrasonic data, which is in agreement with the correlation of estimation errors with the number of speckles.

Results of the F-test for assessing the individual importance of each feature are, in most cases, in agreement with the individual Pearson's correlation coefficients, confirming the observation that the maximum value of the NCX function is the best predictor of displacement estimation errors. For the three lower displacement values, the mean of the 3D gradient magnitude (metric 5), along with the number of speckles (metric 11), seems to be the most promising features. Kurtosis and skewness of the 3D gradient obtained relatively high scores (metrics 8 and 7, respectively).

Application of all of the proposed features to predict the displacement estimation errors using the ensemble regression model significantly improved prediction performance. In the case of separate linear models, the R^2 values reached 0.156 when the maximum of the NCX function was used for the case with a mean displacement of 0.73 mm, and R2 did not exceed 0.08 for the features from groups A through D (see **Table 2**). The multi-variable regression models' maximum R^2 values of 0.532 and 0.524 (for features groups A to E and A to D, respectively) (see **Table 4**) were obtained for the same mean displacement case. They were slightly higher than the 0.15 mm case (0.493 and 0.485).

The influence of reducing the number of features used in the regression training process according to the feature's importance estimated using the F-test differs depending on the mean inter-frame displacement. For lower values (two first cases), the best performance is achieved for 15 or 14 features. Using more than 11 features for higher displacement values does not improve the model. It is essential to keep in mind that the results can be slightly different due to the probabilistic character of ensemble models each time they are trained.

The interpretation of R^2 values in terms of the strength of the prediction varies depending on the application field, but values exceeding 0.5 can be considered moderate or relatively strong.

Conclusions

The conducted study has shown no strong or moderate relationship between the investigated individual kernel features and tracking accuracy and thus none of the examined features is suitable by itself as a criterion for preselecting points of echocardiographic data for further tracking. Neither are any of these features suitable as a means for adjusting the overall echocardiographic imaging settings in order to improve speckle tracking performance. This might be partially explained by the poor feature content of the 3D B-mode data.

When the information available in the whole proposed set of features is combined and fed to a multi-variable regression model, the strength of prediction increases significantly, although the selection of particular features and their number depends at least on the mean interframe displacements (and thus on the used framerate).

Further research involving 2D echocardiographic data and features extracted from the ultrasonic data processing stages earlier than B-mode could provide further insight into the problem and enable more robust selection of tracking points.

References

1. Alessandrini M, Heyde B, Queiros S, et al. Detailed Evaluation of Five 3D Speckle Tracking Algorithms Using Synthetic Echocardiographic Recordings. IEEE Trans Med Imaging. 2016;35(8):1915-1926. https://doi.org/10.1109/tmi.2016.2537848
2. Larsson M, Kremer F, Claus P, Brodin LA, D'hooge J. A novel measure to express tracking quality in ultrasound block matching. 2010 IEEE International Ultrasonics Symposium. 2010;28:1636-1639. https://doi.org/10.1109/ultsym.2010.5935715
3. D'hooge J, Barbosa D, Gao H, et al. Two-dimensional speckle tracking echocardiography: standardization efforts based on synthetic ultrasound data. Eur Heart J Cardiovasc Imaging. 2015;17(6):693-701. https://doi.org/10.1093/ehjci/jev197
4. Jasaityte R, Heyde B, D'hooge J. Current State of Three-Dimensional Myocardial Strain Estimation Using Echocardiography. Journal of the American Society of Echocardiography. 2013;26(1):15-28. https://doi.org/10.1016/j.echo.2012.10.005
5. Lesniak-Plewinska B, Cygan S, Kaluzynski K, et al. A Dual-Chamber, Thick-Walled Cardiac Phantom for Use in Cardiac Motion and Deformation Imaging by Ultrasound. Ultrasound in Medicine & Biology. 2010;36(7):1145-1156. https://doi.org/10.1016/j.ultrasmedbio.2010.04.008
6. Heyde B, Cygan S, Hon Fai Choi, et al. Regional cardiac motion and strain estimation in three-dimensional echocardiography: a validation study in thick-walled univentricular phantoms. IEEE Trans Ultrason, Ferroelect, Freq Contr. 2012;59(4):668-682. https://doi.org/10.1109/tuffc.2012.2245
7. Cygan S, Kumor M, Żmigrodzki J, Leśniak-Plewińska B, Kowalski M, Kałużyński K. Left ventricular phantoms with inclusions simulating transmural and non-transmural infarctions: FEM and EchoPAC study. Duric N, Heyde B, eds. SPIE Proceedings. 2017;10139:1013918. https://doi.org/10.1117/12.2254350
8. De Craene M, Marchesseau S, Heyde B, et al. 3D Strain Assessment in Ultrasound (Straus): A Synthetic Comparison of Five Tracking Methodologies. IEEE Trans Med Imaging. 2013;32(9):1632-1646. https://doi.org/10.1109/tmi.2013.2261823

9. Zmigrodzki J, Cygan S, Wilczewska A, Kaluzynski K. Quantitative Assessment of the Effect of the Out-of-Plane Movement of the Homogenous Ellipsoidal Model of the Left Ventricle on the Deformation Measures Estimated Using 2-D Speckle Tracking—An In-Silico Study. IEEE Trans Ultrason, Ferroelect, Freq Contr. 2018;65(10):1789-1803. https://doi.org/10.1109/tuffc.2018.2856127

10. Wilczewska A, Cygan S, Żmigrodzki J. Segmentation Enhanced Elastic Image Registration for 2D Speckle Tracking Echocardiography—Performance Study In Silico. Ultrason Imaging. 2022;44(1):39-54. https://doi.org/10.1177/01617346211068812

11. Voigt JU, Pedrizzetti G, Lysyansky P, et al. Definitions for a common standard for 2D speckle tracking echocardiography: consensus document of the EACVI/ASE/Industry Task Force to standardize deformation imaging. European Heart Journal - Cardiovascular Imaging. 2014;16(1):1-11. https://doi.org/10.1093/ehjci/jeu184

12. Heyde B, Alessandrini M, Hermans J, Barbosa D, Claus P, D'hooge J. Anatomical Image Registration Using Volume Conservation to Assess Cardiac Deformation From 3D Ultrasound Recordings. IEEE Trans Med Imaging. 2016;35(2):501-511. https://doi.org/10.1109/tmi.2015.2479556

13. Chapelle D, Le Tallec P, Moireau P, Sorine M. An energy-preserving muscle tissue model: formulation and compatible discretizations. Int J Mult Comp Eng. 2012;10(2):189-211. https://doi.org/10.1615/intjmultcompeng.2011002360

14. Hang Gao, Hon Fai Choi, Claus P, et al. A fast convolution-based methodology to simulate 2-Dd/3-D cardiac ultrasound images. IEEE Trans Ultrason, Ferroelect, Freq Contr. 2009;56(2):404-409. https://doi.org/10.1109/tuffc.2009.1051

15. Alessandrini M, De Craene M, Bernard O, et al. A Pipeline for the Generation of Realistic 3D Synthetic Echocardiographic Sequences: Methodology and Open-Access Database. IEEE Trans Med Imaging. 2015;34(7):1436-1451. https://doi.org/10.1109/tmi.2015.2396632

16. Guyon I, Elisseeff A. An introduction to variable and feature selection. J Mach Learn Res. 2003;(3):1157-1182.

17. Wuensch KL, Evans JD. Straightforward Statistics for the Behavioral Sciences. Journal of the American Statistical Association. 1996;91(436):1750. https://doi.org/10.2307/2291607